Electron-phonon interaction, Kohn anomalies, and the Peierls transition in semiconductor quantum wires

J. R. Senna* and S. Das Sarma
Department of Physics, University of Maryland, College Park, Maryland 20742
(Received 24 February 1993)

We calculate the magnitude of phonon softening due to the electron–acoustic-phonon interaction in a continuum one-dimensional model as appropriate for semiconductor quantum wires. We compare the relevant quantum-wire parameters with those of a typical Peierls-unstable one-dimensional compound $K_2Pt(CN)_4Br_{0.3}\cdot 3H_2O$. We obtain quantitative results for the phonon softening, and discuss the possibility of a Peierls instability in quantum-wire structures. We discuss quantitative effects of electron-electron interaction on Kohn anomalies in doped wires. We obtain conditions for a continuous phonon softening as the temperature reaches the mean-field transition temperature. We conclude that for realistic system parameters it is unlikely for quantum wires to exhibit Peierls instability even though strong renormalization of phonon modes may be observable under suitable experimental conditions.

I. INTRODUCTION

Recent advances in nanofabrication have opened up the possibility of making semiconductor wires sufficiently thin for the observation of one-dimensional electron gas (1DEG) behavior.[1] Combining heteroepitaxy and nanolithography one can quantize the motion of the electrons in the conduction band of a semiconductor in two orthogonal directions, while leaving the motion in the third direction essentially free (in the effective-mass sense). Moreover, by controlling the doping of adjacent semiconductor regions and/or the voltage applied to adjacent electrodes, one may be able to continuously vary the concentration of these free carriers. If the combination of (high enough) energy-level spacing due to the lateral confinement and (low enough) carrier concentration is such that only the lowest subband is occupied, the carriers behave as a 1DEG. The construction characteristics of these semiconductor quantum wires, and the relative freedom of choice of material, wire dimensions, and carrier concentrations, make them convenient systems for studying the 1DEG in a jellium background within the effective-mass approximation in a controlled manner.

One task at hand for theory is to ascertain the relevance, for these semiconductor quantum wires of various fundamental results derived earlier in the literature in the context of 1DEG, and observed in other classes of one-dimensional systems. In particular, it was proposed a long time ago by Peierls[2] that 1DEG is inherently unstable with respect to the formation of a ground state consisting of a lattice distortion of wave vector $2k_F$ (k_F=Fermi wave vector of 1DEG) together with a charge-density wave of the electrons of the same $2k_F$ wave vector. In this paper we discuss the relevance of the Peierls instability to semiconductor quantum wires.

The basic concept of the Peierls instability is that in a one-dimensional system the phonon frequency at $2k_F$ may be driven to zero by the electron-phonon interaction effect. Lattice vibrations correspond to a periodic deformation of the lattice. Each lattice deformation causes, through the electron-ion interaction, a change in the energy levels of the electrons. If 1DEG were not polarizable, its energy would increase in regions of dilation and decrease in regions of compression (or vice versa) and the energy to create this distortion would not be altered by the presence of 1DEG. However, 1DEG is polarizable, and responds to the periodic lattice perturbation, redistributing itself to take advantage of the regions where its energy would decrease. The net result is that the restoring force for a lattice deformation is decreased by the presence of 1DEG and, consequently, the vibration frequency lowered. The shift in frequency is expressed by the renormalization of the phonon propagator, whose denominator becomes

$$\hbar^2\omega^2-\hbar^2\omega_q^2-2\hbar\omega_q|M(q)|^2\chi(q,\omega,T)\ , \tag{1}$$

where $\omega_q=cq$ is the bare phonon frequency (i.e., in the absence of 1DEG) at wave vector q, $|M(q)|^2$ is the squared matrix element for the electron-phonon deformation-potential interaction, and χ is the polarizability of 1DEG. In fact, Eq. (1) may have a root $\omega=0$ for $q\neq 0$, and the highest temperature at which this occurs defines the transition temperature T_c for the Peierls instability,

$$\hbar\omega_q+2|M(q)|^2\chi(q,0,T_c)=0\ . \tag{2}$$

The effect is more pronounced in a one-dimensional system for wave vector $2k_F$ (twice the Fermi wave vector) since $\chi(q,0,T_c)$ in 1DEG is strongly peaked at this wave vector and, therefore, $T=T_c$ corresponds to $\omega(2k_F)=0$. Below this temperature, the zero-frequency $2k_F$ mode becomes the static lattice distortion accompanied by the electronic charge-density wave, with the free energy of this distorted configuration lower than that of the undistorted metallic state.

The simple reasoning given above is correct for phonon softening, but not for the occurrence of a phase transi-

tion. If such a transition occurs, it would imply that the continuous translational symmetry of the one-dimensional system would be broken at a nonzero temperature. It is believed that this cannot occur in one dimension if it is driven by a short-range interaction such as the electron-phonon interaction.

There have been several experimental observations of low-temperature phases of this kind in 1D compounds such as tetrafluoro-tetracyanoquinodimethane TF-TCNQ,[3] $NbSe_3$,[4] and $K_2Pt(CN)_4Br_{0.3}\cdot 3H_2O$ (KCP).[5] The stabilization of this Peierls phase has been explained by the intervention of mechanisms for pinning the phase of the charge-density wave. Possible pinning mechanisms could be impurities or interchain coupling between one-dimensional chains. The simple reasoning is believed to give correctly the transition temperature for the onset of the one-dimensional structural fluctuations, which, however, will only stabilize at a lower temperature $T_p < T_c$.[6]

The aim of this paper is to supply quantitative results concerning the softening of acoustic phonons caused by the phonon-1DEG interaction in an artificially structured semiconductor quantum wire, and discuss the possibility of a Peierls instability in such systems. In Sec. II we discuss the interesting general consequences of the continuum model, and in Sec. III we specialize our considerations to semiconductor quantum wires. We conclude with a summary in Sec. IV.

II. PHONON SOFTENING AND PEIERLS TRANSITION

First, it is worth contrasting the characteristics of semiconductor quantum wires with the known Peierls-unstable one-dimensional systems.[7] These are typically "half-filled band" systems, that is, they are be described as a chain of atoms or molecules, with of the order of one free electron per atomic or molecular site, thereby resulting in $k_F b \sim 1$ where b is the lattice spacing. In a semiconductor quantum wire, on the other hand, there are far fewer free electrons than atoms, resulting in $k_F b \ll 1$, the electrons occupying only a small portion of the bottom of the conduction band. The atomic lattice can then be treated as an elastic continuum, and questions concerning the commensurability of the lattice spacing and k_F^{-1} simply do not arise. (Our whole discussion is based on this effective-mass approximation approach to semiconductor quantum wires.)

In the usual Peierls-unstable compounds one can approximate the electron-electron interaction by a short-range interaction, for instance, by an on-site Hubbard repulsion term in a tight-binding model. We define a dimensionless electron density $\tilde{n}$ in terms of the real 1D electron density n and the quantity n^* defined as

$$n^* = \frac{1}{2}\frac{me^2\nu}{\hbar^2\varepsilon_\infty} \tag{3}$$

and

$$\tilde{n} = n/n^* , \tag{4}$$

(where we included a factor ν in the definition of n^* to take care of a possible valley degeneracy in semiconductors, $\nu=1$ for GaAs structures). For dielectric constants ε_∞ of the order of 10, effective-masses m of the order of 0.1, and linear concentrations n of the order of 10^5-10^6 cm^{-1}, $\tilde{n}$ is typically in the range of 1–10 for semiconductor quantum wires, while in the continuum model for the 1D organic compound TF-TCNQ, for instance, would correspond[8] to an electron gas with $\tilde{n}\approx 0.1$. In this sense, the 1DEG in semiconductor quantum wires is a relatively weakly interacting electron gas because the dimensionless densities are substantially higher making kinetic energy relatively more important in quantum wires.

We now apply the simple continuum effective-mass model to 1DEG in a semiconductor quantum wire. We evaluate the changes in the frequency of the acoustic phonons propagating along the quantum-wire axis as described by Eq. (1) and also the temperature T_c given by Eq. (2) as a function of the material parameters of the semiconductor and wire parameters n and a (wire width). The phonons interact with the electrons via the deformation-potential interaction which measures by how much the electron states change in energy for a given amount of strain in the lattice,

$$|M(q)|^2 = \frac{\hbar\Xi^2 q^2}{2\rho a^2 \omega_q} , \tag{5}$$

where ρ is the three-dimensional ionic density and Ξ is the deformation-potential coupling constant for the particular semiconductor. We take into account the electron-electron interaction in 1DEG. Starting from the three-dimensional Coulomb interaction between electrons, one can obtain the matrix element for the interaction between electrons in the lowest subband of a quantum wire (with its axis in the z direction). We get

$$V(q) = \int_{-\infty}^{\infty} dx\, dy\, dx'dy' |\Psi_{00}(x,y)|^2 |\Psi_{00}(x',y')|^2 \times 2K_0(q\sqrt{(x-x')^2+(y-y')^2}) . \tag{6}$$

Here, $\Psi_{00}(x,y)$ is the lowest subband envelope wave function for the electrons. The integration over x's and y's can be done numerically for any model of confinement. For a two-dimensional parabolic confinement the integral involves the two-dimensional harmonic-oscillator ground-state wave function and we approximate the result by

$$V(q) = \frac{2e^2}{\varepsilon_\infty} K_0(qa) , \tag{7}$$

where K_0 is the modified Bessel function of zeroth order.[9]

We introduce some definitions. The material parameters can be grouped as

$$n^* = \frac{me^2\nu}{2\varepsilon_\infty \hbar^2} , \tag{3'}$$

$$M^* = \frac{2}{\pi^2}\frac{\Xi^2 m^2}{\hbar^4 \rho c^2 \varepsilon_\infty} , \tag{8}$$

$$c^* = \frac{16}{\pi}\frac{\hbar c}{e^2}\varepsilon_\infty . \tag{9}$$

TABLE I. Material parameters for some semiconductors. See Refs. 10 and 11.

Material	m (m_0)	ε_∞	ρ (g cm^{-1})	c (10^5 cm s^{-1})	Ξ (eV)	n^* (10^5 cm^{-1})	M^*	c^*
Ge	0.081	16.0	5.32	7.5	11.6	4.8	1.5×10^{-3}	0.28
Si ($\nu=1$)	0.19	12.0	2.33	8.4	13.9	15.0	2.8×10^{-2}	0.23
Si ($\nu=2$)						30.0		
GaAs	0.067	10.9	5.36	4.7	8.6	5.8	2.1×10^{-3}	0.12
GaAs					16.0			

In Table I we display the evaluation of material parameters for some of the best-known semiconductors of technological importance.[10,11] Here, c is the sound velocity in the system.

Then, the quantum wire is characterized by the dimensionless parameters

$$\tilde{a}=an^*/\nu\ , \tag{10a}$$

$$\tilde{n}=n/n^*\ , \tag{10b}$$

$$\tilde{c}=4c/v_F=c^*/\tilde{n}\ . \tag{10c}$$

Other dimensionless quantities are $x=q/2k_F$, $y=\hbar\omega/\varepsilon_F$, $\tilde{D}=D\varepsilon_F$, $\tilde{\chi}=\chi N_F^{-1}$, $t=k_BT\varepsilon_F^{-1}$, and $\tilde{V}=N_FV$, where k_F, ε_F are the Fermi wave vector and energy, N_F is the density of states at the Fermi energy, and k_B is the Boltzmann constant. Then,

$$\tilde{D}=\frac{2\tilde{c}x}{y^2-\tilde{c}^2x^2-\tilde{c}x^2g_1\tilde{\chi}(x,y,t)}\ , \tag{11}$$

$$\tilde{\chi}=\frac{\tilde{\chi}_0}{1-\tilde{V}(x)\tilde{\chi}_0}\ , \tag{12}$$

$$g_1=M^*/\tilde{n}\tilde{a}^2\ < \tag{13}$$

$$\tilde{V}(x)=\left[\frac{4}{\pi}\right]^2\frac{K_0(x\pi\tilde{n}\tilde{a})}{\tilde{n}}\ , \tag{14}$$

and, since we are most interested in the effects at $x=1$ ($q=2k_F$), we define the electron-electron interaction coupling constant by

$$g_2\equiv\tilde{V}(1)\ . \tag{15}$$

The renormalized phonon frequencies are obtained by solving for the roots of the real part of the denominator of the phonon propagator

$$y^2(x)-\tilde{c}^2x^2-\tilde{c}^2x^2g_1\mathrm{Re}\tilde{\chi}[x,y,(x),t]=0\ , \tag{16}$$

and the mean-field equation for the transition becomes (since $\tilde{\chi}_0$ and $\tilde{\chi}$ are purely real for the $y=0$ frequency argument)

$$1+g_1\tilde{\chi}(1,0,t_c)=0\ . \tag{17}$$

We can discuss two interesting consequences of this continuum model in terms of the coupling constants g_1 and g_2, and of the reduced sound velocity $\tilde{c}$, independently of the detailed dependence of these on the material and wire parameters. Using Eqs. (12) and (15), we get

$$1+(g_1-g_2)\tilde{\chi}_0(1,0,t_c)=0\ , \tag{18}$$

so the effect of the Coulomb interaction introduced through the renormalization of the polarizability, Eq. (12), is to decrease the coupling responsible for the transition from the bare value g_1 it would have in Eq. (18) if $\tilde{\chi}$ were approximated by noninteracting $\tilde{\chi}_0$. Since $\tilde{\chi}_0(x,0,t)<0$, this equation will have a solution only if $g_1-g_2>0$. In this case, we can write an explicit solution for t_c by using an analytic approximation[12] for $t\ll1$,

$$\tilde{\chi}_0(1,0,t)=\tfrac{1}{2}\ln(t/4.259),\quad t\ll1 \tag{19}$$

from which

$$t_c=4.259e^{-1/\lambda},\quad \lambda=\frac{g_1-g_2}{2}>0\ . \tag{20}$$

If g_2 were set equal to zero, Eq. (18) for this model would always have a solution with $t_c>0$ because of the divergence of $\chi_0(1,0,t)$ as $t\to0$. This is the essential argument for the intrinsic instability of 1DEG with respect to the Peierls transition; but the simplest effect of the Coulomb repulsion is to introduce a competition and lower t_c, so that for $g_2>g_2$ the complete softening of the $2k_F$ phonons is not allowed, *not even* at T=0.

It is also interesting to consider how the renormalized phonon frequency $y(1)$ behaves as the temperature is lowered. In Fig. 1 we show graphically the solution to the equation

$$y^2-\tilde{c}^2-\tilde{c}^2g_1\mathrm{Re}\tilde{\chi}(1,y,t)=0 \tag{21}$$

for several temperatures. [Actually, in all the numerical calculations x is not set to 1, but to its value at the $\tilde{\chi}(x,0,t)$ peak, which is $x_\mu=\sqrt{\mu/E_F}$ where μ is the chemical potential. This x_μ is approximately equal to 1 for $t\ll1$.] We see that at t_c the zero solution mode appears, but coexisting with a nonzero solution, and below t_c there is a range of t where there are actually two solutions for y. It can be shown[13] that the temperature at which the zero-frequency solution occurs is the same as the one at which lattice deformations begin to appear. In this case, the double roots for $t<t_c$ are probably not physically significant, since in this range of t one should take into account the effect of the deformed lattice. We therefore interpret this as a discontinuous jump at t_c from a nonzero to a zero-frequency mode, and denote this by the dashed line in Fig. 2.

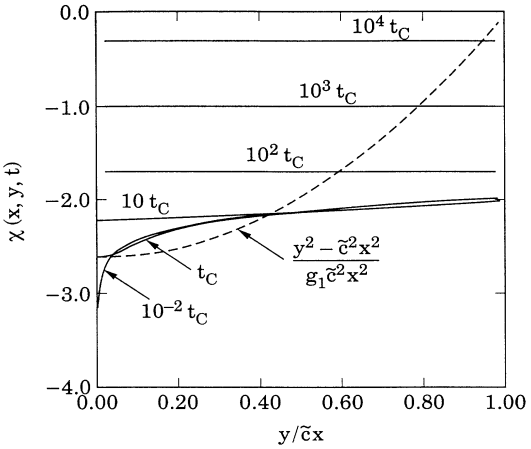

FIG. 1. Graphical depiction of the solution of Eq. (21), for $g_1=0.38$, $g_2=0.17$, and $\tilde{c}=2.3\times10^{-2}$. For these parameters, $t_c=3.8\times10^{-4}$. Solid lines: $\chi(1,y,t)$. Dashed line: $[y^2(1)-\tilde{c}]/g_1\tilde{c}^2$. For this low t_c, $|\chi|$ has developed an acute maximum at $y=0$, so that at and below t_c there are two solutions to that equation. If t_c were higher enough, $\chi(1,y,t_c)$ would still be flatter than the dashed curve, and only one solution for Eq. (21) would result, for all $t>t_c$, and none for $t<t_c$.

It would be interesting to verify whether in this case the order parameter for the deformed lattice (the amplitude of the lattice deformation) also jumps discontinuously from a zero value above t_c to a nonzero value or if it still grows continuously from zero; in any case, we will refer to the discontinuous jump as a first-order transition and the continuous softening as a second-order transition. The present result seems to imply that, if the appropriate parameters are chosen, one could see the appearance of the density fluctuations without observing the complete softening of the $2k_F$ phonon mode.

We can obtain the conditions for the existence of a discontinuity by noting that there is (not) a double root at t_c if the curvature of $\tilde{\chi}(1,y,t_c)$ as a function of y at $y=0$ is bigger (smaller) than the curvature of $(y^2-\tilde{c}^2)/g_1\tilde{c}^2$. From the analytical expansion[14]

$$\tilde{\chi}_0(1,y,t_c)\approx-\frac{1}{(g_1-g_2)}+\frac{y^2}{2t_c^2}\ , \tag{22}$$

we obtain

$$\tilde{\chi}(1,y,t_c)\approx-\frac{1}{g_1}+\frac{(g_1-g_2)^2}{2g_1^2}\frac{y^2}{t_c^2}\ , \tag{23}$$

and using Eq. (20), we obtain that there will be two roots of Eq. (16) for $x=1$ if

$$\tilde{c}>6.40e^{-2/g}\frac{\sqrt{g+g_2}}{g}\ , \tag{24}$$

and only one root ($y=0$) otherwise.

Therefore, in $(g_1,g_2,\tilde{c})$ space one can find a region where the transition is forbidden (the region $g_1<g_2$), another region where the transition is continuous (that is, only a zero-frequency solution at t_c), and a third region where the transition is discontinuous (one zero and one nonzero frequency at $t=t_c$). Te condition expressed in Eq. (24) is represented in Fig. 3 in a g-c diagram where $g\equiv g_1-g_2$. For each value of g_2/g, the curve separating the two regions has a maximum at

$$g=4,\quad \tilde{c}=1.94\sqrt{1+g_2/g}\ . \tag{25}$$

Quite generally, if $g_2<g_1$ the transition is allowed, the effective coupling being g_1-g_2. Even when the transition is allowed, it will occur by a continuous softening of the $2k_F$ phonon as the temperature is lowered only if the electron-phonon coupling (measured by g_1) is large enough or the bare phonon frequency (measured by $\tilde{c}$) is low enough.

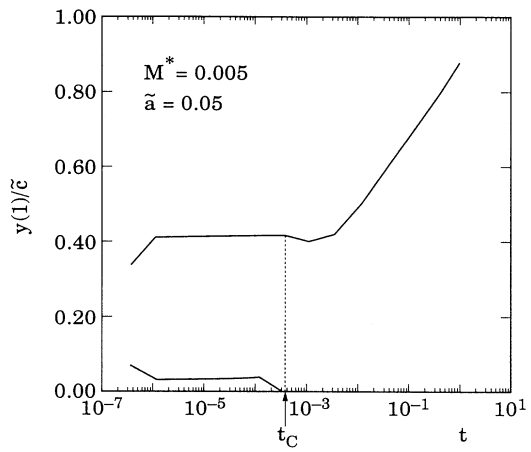

FIG. 2. Roots of Eq. (21) for the same parameters as in Fig. 1. The dashed line indicates the temperature at which the zero-frequency $[y(1)=0]$ solution appears.

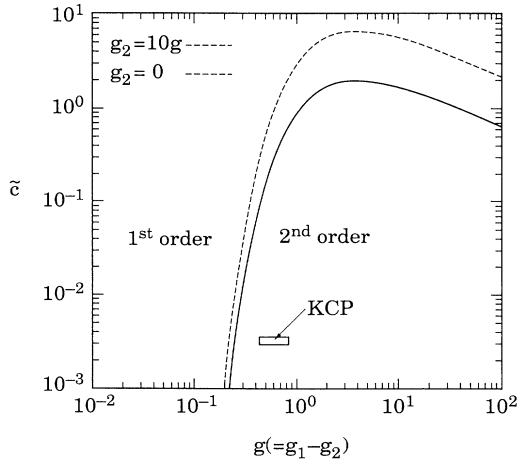

FIG. 3. Regions in $(g,\tilde{c})$ space, characterized by distinct behaviors: the "first-order" region corresponds to the existence of double roots of Eq. (21), as in the example of Fig. 1; the "second-order" region corresponds to the existence of only one root and the $2k_F$ phonon frequency going smoothly to zero as t approaches t_c from above. We have also indicated the region where $(g,\tilde{c})$ for KCP would fall.

This result is quite general, and depends only on the expressions (11) and (12) without any supposition about the dependence of g_1, g_2, and $\tilde{c}$ on material parameters. Let us consider KCP, in which the conduction electrons behave as a 1DEG.[15] Even without a precise estimate of g_2, we see that the right-hand side of Eq. (24) is bigger than its value with $g_2=0$; and the estimates of λ for KCP (Ref. 15) are from 0.2 to 0.4. Therefore, $0.4<g<0.8$ and $6.8\times10^{-2}<6.4\exp(-2/g)g^{-1/2}<5.9\times10^{-1}$, while $\tilde{c}$ is in the range 3×10^{-4} to 4×10^{-4}. So KCP clearly falls in the "second-order" region, and one expects to see a continuous softening of the $2k_F$-phonon mode (which is consistent with the experimental finding).

III. SEMICONDUCTOR QUANTUM WIRES

We now apply these general results to the particular model of semiconductor quantum wires, using Eqs. (10) and (13)–(15). In Fig. 4 we plot λ as a function of dimensionless density $\tilde{n}$, for a particular choice of $\tilde{a}$ and M^*. For $\tilde{n}<\tilde{n}_c$, $g_1<g_2$ and λ becomes negative. This is a manifestation of the first effect described before, and in terms of 1DEG, it corresponds to the electron-electron interaction becoming more important as the density is lowered. Also, there is a maximum at $\tilde{n}=\tilde{n}_0$, the density at which λ has its maximum value λ_0 for given $\tilde{a}$ and m^*. This feature therefore sets an upper limit for t_c for a given wire width and material parameters. If it were not for the electron-electron interaction, one sees from Eq. (13) that no matter how weak the deformation potential, one could always have an arbitrarily large λ (and t_c) by describing the carrier concentration. In Fig. 5 we show the frequency correction $1-y(\tilde{1})/c$ as a function of $\tilde{n}$ for the same parameters. For $\tilde{n}<\tilde{n}_c$ the correction is less than 1, and is bounded by its value at $t=0$,

$$\frac{\Delta(\omega^2)}{\omega^2}=1-\frac{y^2(1)}{\tilde{c}^2}<\frac{g_1}{g_2},\quad \tilde{n}<\tilde{n}_c\ . \tag{26}$$

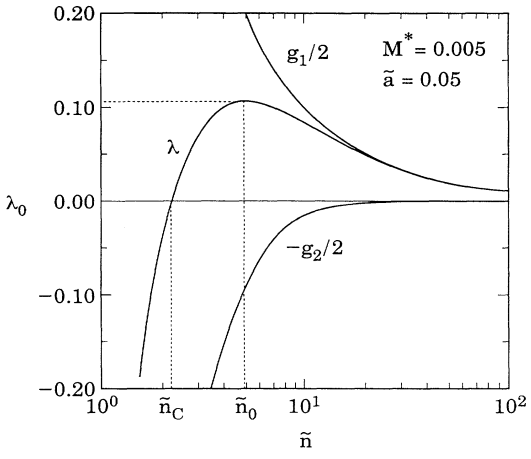

FIG. 4. The coupling constant λ, built from contributions from g_1 (electron-phonon) and g_2 (electron-electron), as a function of dimensionless carrier concentration $\tilde{n}$. The transition is only possible ($\lambda>0$) for $\tilde{n}>\tilde{n}_c$, and at $\tilde{n}=\tilde{n}_0\lambda$ has its maximum value, equal to λ_0.

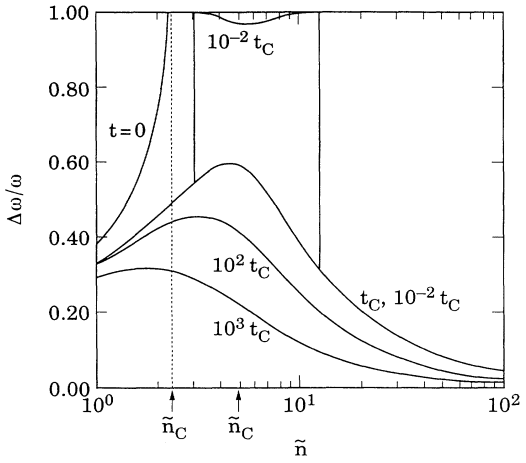

FIG. 5. Relative correction to the $2k_F$ phonon frequency, for the same M^* and $\tilde{a}$, as shown in the figure, for several values of t. For $\tilde{n}<\tilde{n}_c$ the double roots appear, as described in Fig. 1.

For $n>n_c$ the correction reaches 1 for any density at low enough t, with n_0 being the density at which that happens at the highest possible temperature. For $t<t_c$ the double roots described in Sec. II show up in an interval of densities which increases as t is lowered.

It turns out that λ_0 is extremely small for semiconductor quantum wires. From Eqs. (13)–(15) one can obtain $\tilde{n}_0(\tilde{a})$ and $\tilde{n}_0(\tilde{a})$ by solving for the root of $g_1(\tilde{n},\tilde{a})-g_2(\tilde{n},\tilde{a})$ and of its derivative with respect to $\tilde{n}$. We have plotted $\tilde{n}(\tilde{a})$, $\tilde{n}_0(\tilde{a})$, and $\lambda_0(\tilde{a})$ in Fig. 6 for an intermediate value of $M^*=5\times10^{-3}$ and a high value of $M^*=5\times10^{-2}$. We have also tabulated in Table II the numerical values obtained for n_c, n_0, and λ_0 for quantum wires of effective width $a=100$ Å. The resulting values of λ_0 are very small, of the order of 10^{-3} and this rules out an observation of a Peierls instability in these semiconductor quantum wires.

We can also specify our considerations in Sec. II concerning the order of te transition to semiconductor quantum wires using Eqs. (10c), (13), and (14) to translate

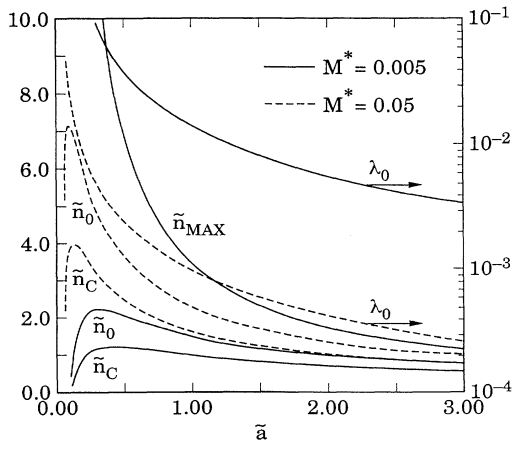

FIG. 6. The quantities $\tilde{n}_c$, $\tilde{n}_0$ (left axis), and λ_0 (right axis), defined in Fig. 5, plotted as a function of $\tilde{a}$.

TABLE II. For the same materials as in Table I, numerical values of the quantities of interest for phonon softening, for an effective width $a = 100$ Å.

Material	$\tilde{a}$ ($a = 100$ Å)	n_c (10^6 cm^{-1})	n_0 (10^6 cm^{-1})	$\tilde{c}(\tilde{n}_0) = c^*/n_0$	$g_1(n_0,a)$	$g_2(n_0,a)$	$\lambda_0(a)$
Ge	0.48	1.6	2.2	6.1×10^{-2}	1.4×10^{-3}	1.7×10^{-4}	6.3×10^{-4}
Si ($\nu=1$)	1.5	1.4	2.0	1.7×10^{-1}	9.5×10^{-3}	1.2×10^{-3}	4.1×10^{-3}
Si ($\nu=2$)	1.5	2.8	3.9				
GaAs	0.58	1.6	2.2	3.2×10^{-2}	1.6×10^{-3}	2.0×10^{-4}	7.2×10^{-4}
GaAs		1.2	1.8	3.9×10^{-2}	6.9×10^{-3}	9.8×10^{-4}	3.0×10^{-3}

those phase diagrams into a dependence on the wire parameters $\tilde{a}$, $\tilde{n}$, and $\tilde{c}$ and material parameters M^*, c^*, and n^*. This is shown in Fig. 7, where in addition to the $\tilde{n}_c(\tilde{a})$ curve separating the "no transition" and "transition" regions, there is a curve, obtained from the "first-order" or "second-order" regions.

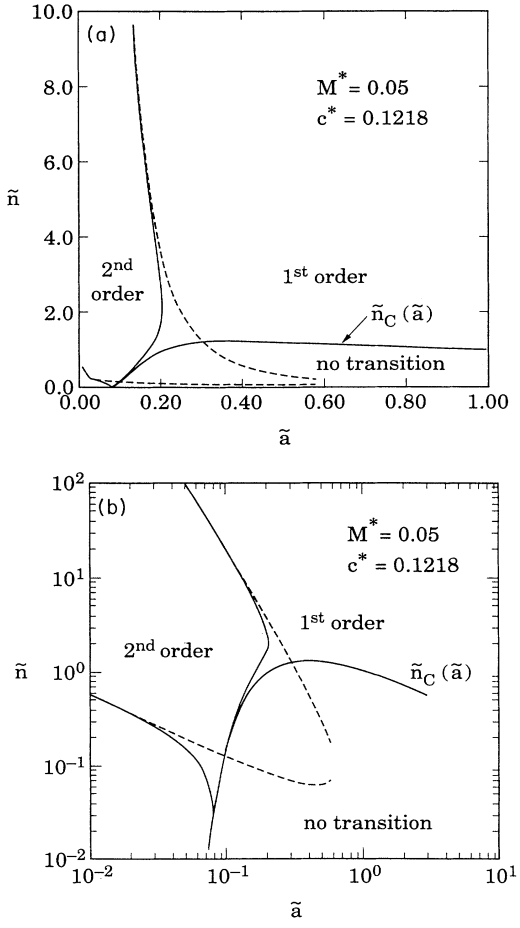

FIG. 7. (a) Conditions for the existence or not of transition, and for the occurrence ("first order") or not ("second order") of double roots of Eq. (21), in terms of quantum-wire parameters: density of carriers $\tilde{n}$ and effective width $\tilde{a}$. The "no transition" region is delimited by the same $\tilde{n}_c(\tilde{a})$ shown in the figure; the "second-order" region corresponds to the large effective coupling constant. The dashed curve represents the frontier between the "second-order" and "first-order" regions when the electron-electron interaction is set to zero; the solid curves were obtained with $\tilde{V}$ for GaAs material parameters. (b) Detail.

It is unlikely that in real semiconductor quantum wires the phonon anomaly can ever become large enough to lead to a complete softening. There can, however, be significant corrections to the phonon frequency (Kohn anomaly) which may affect te electronic transport properties. We show numerical results for GaAs quantum wires. Because of the uncertainty in the literature concerning the value of the electron-LA phonon deformation potential, we present numerical results for $\Xi = 7.0$ eV, a conservative estimate. (Results for other values of Ξ can be obtained by a simple rescaling.) The normalized phonon frequencies are given by the solution of Eq. (16). In Figs. 8(a) and 8(b) we show the relative corrections for

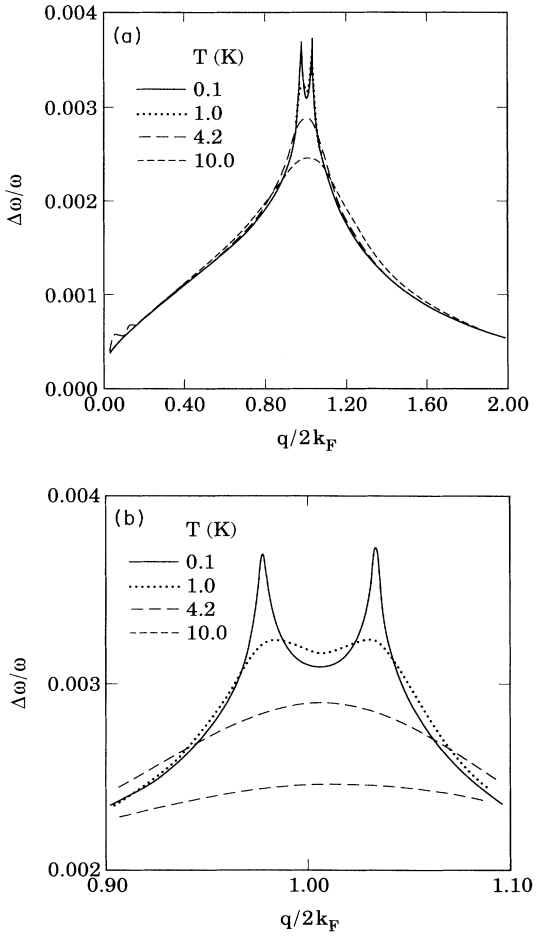

FIG. 8. (a) Kohn anomaly for GaAs quantum wire of effective width $a = 100$ Å, for several temperatures. (b) Detail.

temperatures between 10 and 0.1 K. Because of the smallness of the phonon renormalization one can write the approximation

$$\frac{\Delta\omega}{\omega} \approx -\frac{g_1}{2}\mathrm{Re}\tilde{\chi}(x,\tilde{c}x,t) \ . \tag{27}$$

So, the shape of the relative correction, as a function of x, is similar to that of the polarizability at the bare phonon frequency. Correspondingly, there is a double-peaked structure noticeable at lower temperatures, and smeared at higher temperatures. The peaks are located approximately at $x=1\pm\tilde{c}/4$, and disappear when the temperature is comparable to the splitting. It is worth noting that it is not, in general, a good approximation to replace χ on the right-hand side of Eq. (26) by its static value as is sometimes done in the context of higher dimensional systems. In this case, not only that the peak structure is lost, but referring back to Fig. 1, one sees that the static approximation may give a large overestimate of the correction. Since for a 1DEG, electronic transport at $t \ll 1$ can only be limited by $2k_F$ ($x=1$) scattering, it is important to use the correct form of the renormalization.

The magnitude of the correction can also be calculated for a given x as a function of carrier concentration n and width a. We expect a maximum as we had for λ. Some representative results are shown in Fig. 9. It is important to notice that these results are given for a constant temperature T (and therefore varying $t=k_BT/E_F$) instead of a constant t as in Fig. 6.

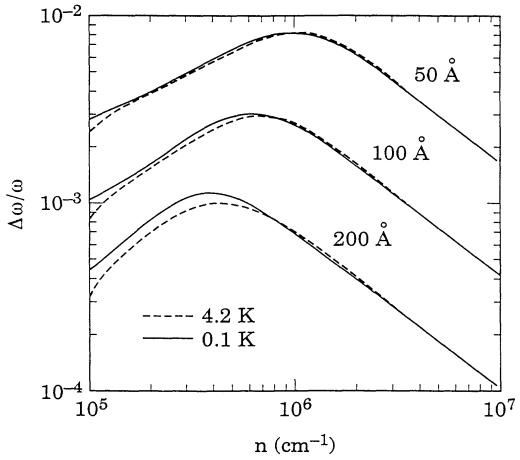

FIG. 9. Relative phonon frequency correction at $2k_F$ for GaAs quantum wire, as a function of carrier concentration, for constant temperature T. The magnitude of the correction increases approximately with $(\text{width})^{-2}$, reflecting the dependence of the coupling g_1 on a.

IV. SUMMARY AND CONCLUSIONS

We have shown that the simple picture of a phonon softening-driven Peierls transition in 1DEG has some interesting consequences in the presence of the electron-electron interaction: the existence or not of a transition is controlled by an effective coupling corresponding to the quantitative difference between electron-phonon and electron-electron interactions, and the competition between the strengths of the effective coupling and the bare phonon frequency controls whether the softening is continuous or not. We have applied these results to an effective-mass model of semiconductor quantum wires, and ascertained that the effective coupling for realistic quantum-wire parameters is too weak for an experimentally observable Peierls transition. There may very well be significant renormalization of phonon frequencies in quantum wires and we have calculated the magnitude of this Kohn anomaly for realistic system parameters. We have neglected the effect of static disorder arising from random impurities in the system. In general, the Kohn anomalies will be weaker in strongly disordered systems.

ACKNOWLEDGMENTS

One of the authors (S.D.S.) thanks Professor Rudolf Peierls for a very illuminating discussion. This work was supported by the U.S.-ARO, the U.S.-ONR, and the MT-DMR program of the NSF. J.R.S. acknowledges support from CNPq (Brazil).

*On leave from Instituto Nacional de Pesquisas Espaciais-INPE, Caixa Postal 515, 12201-São José dos Campos, São Paulo, Brazil.

[1]For reviews, see, for instance, *Nanostructures and Mesoscopic Systems,* edited by Wiley P. Kirk and Mark A. Reed (Academic, Boston, 1992); *Electronic Properties of Two-Dimensional Systems,* Proceedings of the EP2DS-9 Conference, edited by M. Saitoh (Yamada Science Foundation, Japan, 1992); *Solid State Physics: Semiconductor Heterostructures and Nanostructures,* edited by H. Ehrenreich and D. Turnbull (Academic, Boston, 1991), Vol. 44.

[2]R. E. Peierls, *Quantum Theory of Solids* (Clarendon, Oxford, 1955).

[3]S. Kagoshima, H. Anzai, K. Kajimora, and T. Ishiguro, J. Phys. Soc. Jpn. **39**, 1143 (1975).

[4]K. Tsutsumi, T. Takagaki, M. Yamamota, Y. Shizaki, M. Ido, T. Sambongi, K. Yamaya, and Y. Abe, Phys. Rev. Lett. **34**, 1675 (1977); R. M. Fleming, D. E. Moncton, and D. B. McWhan, Phys. Rev. B **18**, 5560 (1978).

[5]R. Comes, M. Lambert, H. Launois, and H. R. Zeller, Phys. Rev. B **8**, 571 (1973).

[6]Jean Paul Pouget, in *Low-Dimensional Conductors and Superconductors,* edited by D. Jérome and L. G. Caron (Plenum, New York, 1987), p. 17.

[7]S. Kagoshima, H. Nagasawa, and T. Sambogi, *One-Dimensional Conductors* (Springer, New York, 1987).

[8]We obtain this by using $m=3m_0$ (Ref. 6, Chap. 3) and $e_\infty=1$ to obtain $n^*=2.8\times10^8$ cm^{-1}, and $k_F=4.8\times10^7$ cm^{-1} (Ref. 6, Chap. 3) to obtain $n=2k_F/\pi=3.1\times10^7$ cm^{-1}.

[9]The exact form of $V(q)$ will depend on the choice of confinement model [i.e., of $\Psi_{00}(x,y)$]. See, for example, S. Das Sarma and W. Y. Lai, Phys. Rev. B **32**, 1401 (1985). Ex-

plicit numerical calculations, using different confinement models (square and triangular confinement) show that the $K_0(qa)$ asymptotic form of this matrix element remains valid qualitatively for large q as well. While we do not expect parabolic confinement to produce an exact $K_0(qa)$ matrix element, we can always invert the problem and take the confinement to be such that the matrix element is given *exactly* by $K_0(qa)$. Clearly, this can be done with no loss of generality, since the specific confinement for quantum wires will depend on the details of fabrication. The form used here is more convenient for numerical calculations.

[10]The estimates were made using low-temperature data reported in Ref. 11, and taking as direction z of the wire and of propagation of the LA phonons a light mass axis of the conduction-band constant-energy ellipsoids. Then the mass m is the transverse mass of the ellipsoid. For Si we take z to be (100), and the effective deformation potential is $\Xi=\Xi_d+\Xi_u$; for Ge we take z to be (1−10), and $\Xi=\Xi_d+\Xi_u/6$; for GaAs we suppose a parabolic conduction band and $\Xi=\Xi_d$, and we use both a low estimated value of $\Xi_d=8.6$ eV and a high estimated value of $\Xi_d=16$ eV. In Si, from elementary considerations, one would expect a valley degeneracy $\nu=2$ for (100) wires; however, perturbations can raise this valley degeneracy, and so we present results for $\nu=1$ and $\nu=2$.

[11]*Numerical Data and Functional Relationships in Science and Technology,* edited by O. Madelung, Landolt-Börnstein, New Series, Group III, Vol. 17, Pt. a (Springer, Berlin, 1982).

[12]This can be obtained by approximating the Fermi function in the Lindhardt expression for χ_0 by a piecewise linear function; see, for instance, B. Horowitz, M. Weger, and H. Gutfreund, Phys. Rev. B **9**, 1246 (1977). We obtained the numerical coefficient of t in this equation by fitting this form to the numerically evaluated $\tilde{\chi}$.

[13]*One-Dimensional Conductors* (Ref. 7), p. 14.

[14]Again using the analytical approximation of Horowitz *et al.* (Ref. 12), and expanding to lower order in y/t.

[15]P. Bruesch, *Phonons: Theory and Exeriments III* (Springer, New York, 1982), Chap. 5.